Hindawi
Journal of Renewable Energy
Volume 2019, Article ID 5168259, 15 pages
https://doi.org/10.1155/2019/5168259

Research Article

Experimental Characterisation of Photovoltaic Modules with Cells Connected in Different Configurations to Address Nonuniform Illumination Effect

Damasen Ikwaba Paul

Physical Sciences Department, Faculty of Science, Technology and Environmental Studies, The Open University of Tanzania, P.O. Box 23409, Dar es Salaam, Tanzania

Correspondence should be addressed to Damasen Ikwaba Paul; paul.ikwaba@out.ac.tz

Received 16 October 2018; Accepted 5 March 2019; Published 1 April 2019

Academic Editor: Abhijeet P. Borole

Most concentrating systems that are being used for photovoltaic (PV) applications do not illuminate the PV module uniformly which results in power output reduction. This study investigated the electrical performance of three PV modules with cells connected in different configurations to address nonuniform illumination effect. PV module 1 is the standard module consisting of 11 solar cells connected in series whereas PV module 2 is a proposed design with 11 cells in three groups and each group consists of different cells in series connections. PV module 3 is also a new design with 11 cells in two groups and each group consists of different cells connected in series. The new PV modules were designed in such a way that the effect of nonuniform illumination should affect a group of cells but not the entire PV module, leading to high power output. The PV modules were tested under three different intensities: uniform, low nonuniform, and high nonuniform illumination. When the PV modules were tested at uniform illumination, the total maximum power output of PV module 1 was higher than that of PV module 2 and PV module 3 by about 7%. However, when the PV modules were tested at low nonuniform illumination, the total maximum power output of PV module 2 was higher than that of PV module 1 and PV module 3 by about 4% and 7%, respectively. This difference increased to about 12% for PV module 3 and 17% for PV module 1 when the modules were tested at high nonuniform illumination. Therefore, the best PV module design in addressing nonuniform illumination effect in solar collectors is PV module 2. In practical situation this implies that manufacturers of PV modules should consider designing modules with groups of cells in series connection instead of all cells being connected in series.

1. Introduction

The demand of solar electricity as a clean energy is increasing but its generation is limited by the cost of the photovoltaic (PV) modules [1, 2]. The reason is that over half of the total cost of the solar electricity system is spent on purchasing the PV modules [1]. The use of solar concentrators offers a solution to this problem since concentrating systems increase solar flux density on the PV module and hence give high electricity in comparison with similar nonconcentrating system [1, 3, 4]. Thus, a significant reduction is made in the cost of the PV system because the amount of expensive semiconductor materials are reduced [1, 3, 4]. However, the power output of a PV module with a concentrator increases if and only if the radiation is distributed uniformly across the entire PV module. Unfortunately, most concentrating systems that are being used for solar electricity generation such as Compound Parabolic Concentrators (hereafter called CPCs), parabolic trough, and Fresnel lens do not illuminate the PV module uniformly which results in power output reduction [5–9]. The reason is that under nonuniform illumination the least illuminated PV cells (which produce less current) are also forced to carry high current similar to the other fully illuminated cells [9]. As a result, the least illuminated PV cells get reverse biased and drain power from the fully illuminated cells and this leads into "hot spots" [9–14]. For conventional PV modules such hot spots cause reduction in the power output since the entire PV module

depends on the least illuminated PV cell(s) [10–14]. In this case, high energy concentrations above the least illumination cells do not contribute to power generation, thus limiting the application of concentrators in photovoltaic applications. In addition, nonuniform illumination causes nonuniform temperature profiles among the cells in the PV module, leading to further reduction in maximum power output and electrical conversional efficiency [7, 12, 15].

Over the past four decades, the CPC has been the most popular static low-concentrating system for PV application [4, 16, 17]. The CPC is a nonimaging ideal collector as it attains the highest possible concentration of radiant energy permitted by the second law of thermodynamics [18]. The main advantages of CPCs over other solar collectors include high optical efficiency [18], minimum errors of alignment [19], elimination of the diurnal tracking requirement at intermediate concentrations (up to 10×) [18], and being able to collect both diffuse and direct radiation [18–21]. Generally, CPCs are categorised as two-dimensional (2D) [18, 19, 21] or three-dimensional (3D) collectors [18, 19, 22]. The former may be further classified as symmetric CPC [18, 19] or asymmetric CPC [18]. However, most CPCs do not illuminate the receiver uniformly [6–8, 15]. The illumination profiles on the PV module with symmetric 2D CPC has been studied in detail by Zacharopoulos et al. [23] and Paul [8] while Sarmah et al. [24] and Lie et al. [25] have presented the illumination characteristics for the asymmetric CPCs.

In an effort to ensure that the cost of the PV-CPC systems is cheaper than the conventional flat systems, different techniques have been proposed to eliminate the effect of nonuniform illumination in the CPCs. The first attempt was done by Gupta et al. [26] who used an exact mathematical expression to design the reflecting surfaces of the symmetric 2D CPC which would illuminate the PV module uniformly. Their theoretical and experimental results showed that the illumination on the rectangular PV module was uniform to within 10 to 12%. Yu et al. [27] proposed a CPC called restricted exit angle in which the upper part consisted of a parabolic section whilst the lower part had a straight section. Their simulation results indicated that the straight section had a significant influence on the uniformity and the intensity distribution became more uniform with the decrease of the restricted exit angle. Zhang et al. [28] proposed a novel biaxial tracking CPC with a special truncation called "Well Distributed CPC" (WD-CPC). It was found that the nonuniformity of the WD-CPC decreased to about 27% of a common CPC.

Another technique of attaining energy flux uniformity on the surface of the PV module is the use of diffuse reflector materials in fabricating the concentrators. The first attempt was done by Nilsson et al. [30] who evaluated the illumination patterns of three different structured reflectors (120° V-shape, 60° V-shape, and sinusoidal shape). Their results showed that all three reflectors reduced considerably the peak intensity of the light incident on the PV module but sinusoidal microstructure had the best effect. Hatwaambo et al. [31] examined the nature of the energy flux distribution of two highly specular materials (miro and anodized aluminium) and a diffuse material with rolling marks (rolled aluminium foil). Experimental results showed that the energy flux distribution was more uniform with the diffuse rolled aluminium reflector than highly specular materials. Based on the previous study, Hatwaambo et al. [32] carried out another study on the use of semi-diffuse rolled reflective elements. The analysis involved two identical symmetric 2D CPCs: one with the diffuse rolled aluminium sheet with its rolling grooves aligned parallel to the plane of the PV cell and the other CPC with the same diffuse rolled aluminium sheet but in this case the rolling marks aligned perpendicular to the plane of the PV cell. Their experimental results indicated that a semi-diffuse aluminium sheet reflector with rolling grooves oriented parallel to the plane of the PV cell scattered the radiation evenly than when the rolling marks were aligned perpendicular to the plane of the PV cell. Similar conclusion was made by Hatwaambo [33]. Simfukwe et al. [34] studied experimentally the effect of using locally available low-cost semi-diffuse reflectors in addressing nonuniformity challenge. Four different semi-diffuse structured aluminium reflectors were investigated, namely, plain sheet, horizontal grooves, vertical grooves, and crisscross grooves. They found that the crisscross groove and the horizontal groove orientation were the best orientations as they scattered the solar energy flux more uniformly across the PV module. Esparza and Moreno [35] experimentally examined the use of a diffuser segment on top and bottom of the CPC reflectors. It was found that energy flux distribution was more uniform for CPCs with diffusers than similar CPC without a diffuser. It was further found that the location of the diffuser was also important as the CPC with a diffuser segment at the bottom produced a more uniform irradiance than a CPC with the diffuser at the top.

The optical mixer is another technique for improving the nonuniform illumination in solar collectors. Parretta et al. [36] used a prismatic optical mixer at the exit aperture of a 3D CPC and found that with a properly dimensioned prismatic optical mixer, light was uniformly distributed on the solar cell. The use of bypass diode is also another technique that has been used to improve the performance of the PV module under nonuniform illumination as discussed by Fernandes et al. [37]. The design of special PV cells is another technique that has been used to eliminate the effect of nonuniform illumination. Paul et al. [7] proposed the use of isolated cells PV module. In their study, the analysis confirmed that the PV module with individual cells and the effect of nonuniform illumination results in high power output for cells located in the peak energy concentration regions and low power output for cells in the lower illumination areas. On the other hand, Paul and Smyth [38] designed and fabricated a novel hybrid PV cell consisting of high efficiency and low efficiency cells. Their experimental results indicated that the overall daily power output of the hybrid PV cell was higher than that of similar conversional PV cell by 12%.

Another way of mitigating nonuniform illumination effect in PV application is the use of planar concentrators such as the V-trough which illuminate the receiver more uniformly than the CPCs [39–42]. However, the application of V-trough collector in photovolitaics is limited by the low concentration ratio [40–43].

In this study, special designs of PV modules with cells connected in different configurations to address nonuniform illumination effect in solar collectors are proposed. Three different PV modules designs have been examined in this work. PV module 1 is the standard module consisting of 11 solar cells connected in series (which acts as a reference) whereas PV module 2 is a new proposed design with 11 cells in three groups and each group consists of different cells connected in series. PV module 3 is also a new design with 11 cells in two groups and each group consists of different cells connected in series. The proposed PV modules were designed in such a way that the effect of nonuniform illumination should affect a group of cells but not the entire PV module, which means maximum power output from the whole PV module. The electrical performance of the three PV modules was analysed under three different solar radiation conditions: uniform illumination, low nonuniform illumination, and high nonuniform illumination.

2. Materials and Methods

2.1. Design and Fabrication of the Photovoltaic Modules. In this study, three different photovoltaic modules (PV module 1, PV module 2, and PV module 3), each consisting of 11 solar cells, were designed and fabricated. The fundamental difference between these PV modules lies on the solar cells connections as illustrated in Table 1 and Figure 1. Each PV module was fabricated by using monocrystalline BP Saturn (9 mm wide) solar cells with specifications shown in Table 2 [43].

In fabricating the PV modules, Perspex with 11 rectangular space blocks was used as shown in Figure 1. The function of the rectangular space blocks was to allow each cell to sit between the rectangular edges to avoid dislocation and short circuiting between each cell. A connector board that facilitates the PV cells to be connected in different combinations was fixed at the rear side of the Perspex base using both M2 screws and Araldite 2011B adhesive. For the purpose of measuring the back-surface temperature of each cell, holes were drilled to the middle of the Perspex to enable thermocouple to be attached to the rear surface of each cell.

2.2. Design and Fabrication of the Solar Collectors. The aim of this paper was to experimentally characterise the PV modules fabricated in Section 2.1 under uniform and nonuniform solar radiation illumination. The uniform solar radiation illumination was achieved by testing the PV modules without concentrating system whilst nonuniform illumination was created by testing the PV modules with the V-trough collector and the CPC. The choice of these concentrators was based on the energy distribution profiles of each collector [8]. The V-trough collector was used to create low nonuniform energy flux distributions on the PV module whilst the CPC was used to obtain high nonuniform energy flux distributions on the PV module. Therefore, a V-trough collector (Figure 2(a)) and a symmetric 2D CPC (Figure 2(b)) were designed according to the parameters in Table 3. Each concentrator was designed in such a way that the PV module (with dimensions shown in Figure 1) fits exactly on the receiver area. Both concentrators were fabricated with high reflectivity anodised aluminium sheets with reflectivity of 0.91.

2.3. Experimental Test Procedure and Set up

2.3.1. Experimental Test Procedure. In order to control the amount of illumination intensity in each experiment, indoor experimental testing was used in this study. Each of the three fabricated PV module was tested at three different solar illumination conditions: without a concentrating system (uniform illumination), with the V-trough collector (low nonuniform illumination), and with the CPC (high nonuniform illumination). These indoor experimental tests were carried out using a multipurpose mobile solar simulator [29]. The multipurpose mobile solar simulator uses metal halide lamps (Osram HMP575W) with a good spectral match to AM1.5 standard solar spectrum as shown in Figure 3. This simulator has a lamp-frame height which can be adjusted depending on the requirement of the experiment. Thus, the light uniformity of the multimobile solar simulator also varies with target area and lamp-frame distances. For example, at a height of 1.8 m (from the target), the uniformity of about 94% can be achieved on a 2.2 m × 1.5 m wide target area while, at a distance of 2.2 m from the lamp array, the uniformity decreases to about 90% [29].

For each experimental test, a constant solar illumination of 600 W/m^2 was set to illuminate the test unit and was measured by using Kipp and Zonen pyranometer with directional error of less than ±20 W/m^2 at 1000 W/m^2 [44]. For the purpose of measuring temperature, a total of 12 thermocouples were used; 11 for measuring the temperature of the 11 cells in the PV module and one thermocouple for measuring the ambient temperature. All the thermocouples were connected to a Data-Logger and programmed to take measurements every 10 seconds and average the results every 30 seconds. For each experimental test, the temperature was kept constant to nearly that of the ambient temperature by using a fan. The current and voltage of each PV module was measured with Keithley 2400 SourceMeter. The Keithley 2400 Model SourceMeter has the following instrumental error: DC voltage: ±0.8 mV for 2.0 V range and DC current: ±2.8 mA for 1.0 A range [45].

From the current and voltage measurements, the current-voltage (I–V) curves were plotted. These curves were used to extract the open-circuit voltage (V_{OC}), short-circuit current (I_{SC}), current at maximum power point (I_{MPP}), voltage at maximum power point (V_{MPP}), and maximum power output (P_{MPP}). The fill factor (FF) of each PV module was calculated from [46]

$$FF = \frac{I_{MPP} \times V_{MPP}}{I_{SC} \times V_{OC}} = \frac{P_{MPP}}{I_{SC} \times V_{OC}} \quad (1)$$

2.3.2. Experimental Set up. For each experiment, the test unit (PV module without collector, PV module with the V-trough, and PV module with the CPC) was mounted horizontally at the centre of the solar simulator and positioned so that the illumination was always perpendicular to the test unit. This

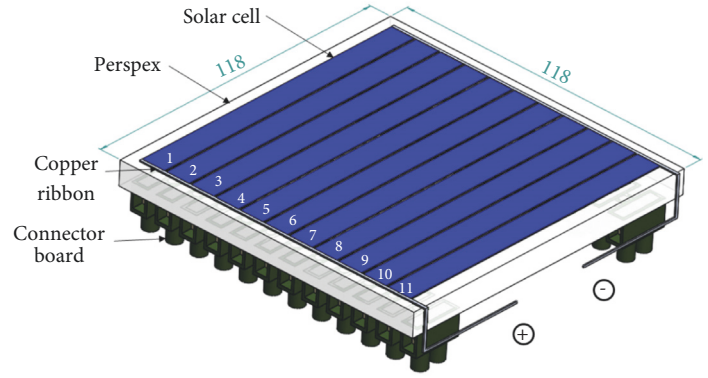

Solar cell numbers 1 to 11 are connected in series.

(a) PV module 1

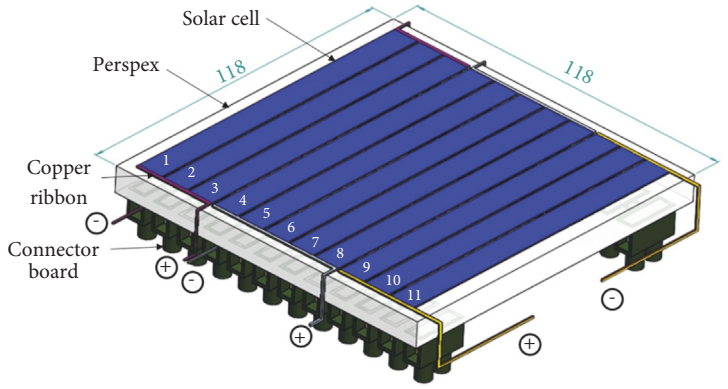

The PV module consists of three blocks:

- Block 1 (purple colour): Solar cell numbers 1, 2, and 3 are connected in series.
- Block 2 (white colour): Solar cell numbers 4, 5, 6, 7, and 8 are connected in series.
- Block 3 (yellow colour): Solar cell numbers 9, 10, and 11 are connected in series.

(b) PV module 2

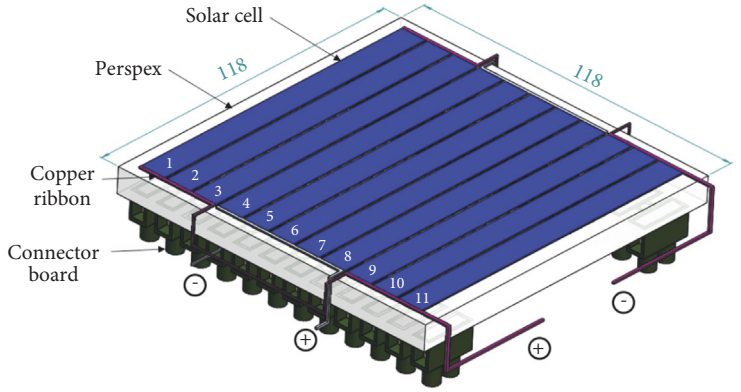

The PV module consists of two blocks:

- Block 1 (purple colour): Solar cell numbers 1, 2, 3, 9, 10, and 11 are connected in series.
- Block 2 (white colour): Solar cell numbers 4, 5, 6, 7, and 8 are connected in series.

(c) PV module 3

Figure 1: Different solar cells connections in the PV modules (all dimensions in mm).

setting allowed maximum solar irradiance to be received on the aperture of the test unit.

To examine the effect of solar radiation incidence angle on the performance of the proposed PV modules, each test unit (under the three illumination conditions: without collector, with the V-trough, and with the CPC) was tilted manually to different incidence angles. Due to angular acceptance limits of the solar collectors (indicated in Table 3), each test unit was titled between 0° and 21° at an interval of 5°. Figure 4 shows an example of a test unit (PV-CPC) tilted to 15° from the perpendicular of the aperture. For each incidence angle and each experimental test, V_{OC}, I_{SC}, I_{MPP}, V_{MPP}, and P_{MPP} were extracted from the I–V curves. The FF of each PV module at that incidence angle was calculated using (1).

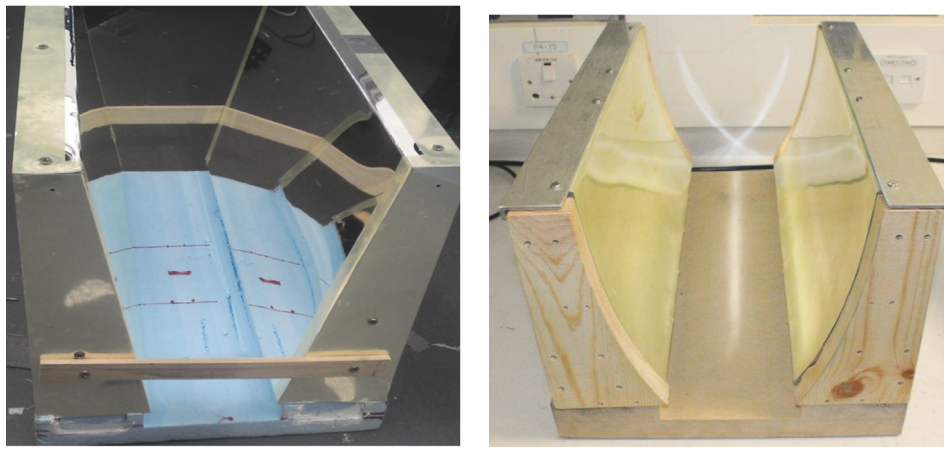

(a) (b)

Figure 2: Fabricated solar collectors (a) V-trough collector, (b) symmetric 2D CPC.

Table 1: Design characteristics of each PV module.

Types of the PV module	PV cell used in the fabrication	Dimensions (length × width × depth) of the PV cell (in mm)	Total number of PV cells in the module	PV cells connections	Design illustration
PV module 1	Solar Saturn	109 × 9 × 0.4	11	All 11 cells connected in series	Figure 1(a)
PV module 2	Solar Saturn	109 × 9 × 0.4	11	The PV module consists of three blocks with cells connected as follows: (i) Cell Nos. 1, 2, and 3 connected in series (ii) Cell Nos. 4, 5, 6, 7, and 8 connected in series (iii) Cell Nos. 9, 10, and 11 connected in series	Figure 1(b)
PV module 3	Solar Saturn	109 × 9 × 0.4	11	The PV module consists of two blocks with cells connected as follows: (i) Cell Nos. 1, 2, 3, 9, 10, and 11 connected in series (ii) Cell Nos. 4, 5, 6, 7, and 8 connected in series	Figure 1(c)

3. Results and Discussions

3.1. Electrical Performance Analysis of the PV Modules under Uniform Illumination. This section presents the results from the analysis when the PV modules were tested under uniform illumination condition.

3.1.1. Comparison of Open-Circuit Voltage. Figure 5 compares the open-circuit voltage of each PV module under uniform illumination for difference solar incidence angles. Although all the PV modules had the same number of solar cells, it can be seen that the open-circuit voltage of PV module 1 was higher than that of PV module 2 and PV module 3 by about 8% at each incidence angle. This is explained by the size or area of the solar cells connected in series. As illustrated in Figure 1, all solar cells are connected in series in PV module 1 (Figure 1(a)) while there are three groups of cells in series connections in PV module 2 (Figure 1(b)) and two groups of cells in series connection in PV module 3 (Figure 1(c)). This implies that the area of the solar cells connected in series in PV module 1 was bigger than that in PV modules 2 and 3. It has been found that PV modules with small surface area exhibit high values of reverse saturation current density (J_0) than similar module with large area [47, 48] and

Table 2: The specifications of the 11 BP Saturn solar cell used in the current study. These electrical data apply for 800 W/m^2 solar irradiance, average cell temperature of 18°C, AM[1]1.5 spectrum, and ambient temperature of 20°C [43].

	Cell No.	I_{SC}[2] (mA)	V_{OC}[3] (V)	P_{MPP}[4] (mW)	FF[5] (%)	η[6] (%)
Cell specification	1	240.20	0.58	80.74	57.95	10.29
	2	240.90	0.58	79.57	56.95	10.14
	3	244.72	0.59	83.38	57.75	10.62
	4	248.14	0.59	82.61	56.43	10.53
	5	242.61	0.59	77.39	54.07	9.86
	6	241.79	0.59	81.79	57.34	10.42
	7	246.58	0.59	85.03	58.45	10.84
	8	245.96	0.59	85.19	58.71	10.86
	9	246.53	0.59	84.31	57.96	10.74
	10	244.79	0.59	77.90	53.93	9.93
	11	240.85	0.59	82.05	57.74	10.45
	Average	*243.92*	*0.59*	*81.81*	*57.02*	*10.30*

[1] AM is air mass
[2] I_S is short-circuit current
[3] V_{OC} is open-circuit voltage
[4] P_{MPP} is power output at maximum power point
[5] FF is the fill factor
[6] η is solar cell conversion efficiency

Table 3: Geometrical dimensions of the 2D CPC and V-trough collector.

Parameter	CPC (before truncation)	CPC (after truncation)	V-trough
Acceptance half-angle (°)	30.0	30.7	21.0
Trough angle (°)	[-]	[-]	10.0
Concentration ratio [-]	2.0	1.96	1.96
Aperture width (mm)	218.0	213.64	213.64
PV module width (mm)	118.0	118.0	118.0
PV module length (mm)	118.0	118.0	118.0
PV module active area (mm)	109 × 109	109 × 109	109 × 109
Maximum height (mm)	282.4	212.07	296.72
Collector maximum length (mm)	500.0	500.0	500.0

therefore have low open-circuit voltage according to equation (2) [49–51]. Equation (2) shows that the smaller the value of J_0 of a PV module, the higher the open-circuit voltage. Thus, an increase in J_0 produces a reduction in V_{OC} proportional to the inverse of the logarithm of the increase.

$$V_{oc} = \frac{k_B T}{q} \ln\left(\frac{J_{ph}}{J_o} + 1\right) \approx \frac{k_B T}{q} \ln\left(\frac{J_{ph}}{J_o}\right) \quad (2)$$

where k_B is Boltzmann's constant, T is absolute temperature, q is absolute value of the electron charge, and J_{ph} is photocurrent density.

Figure 5 also shows that the open-circuit voltage of each PV module remained constant despite of the fact that the incidence angles were varied significantly. The main reason is that since the PV module was very small (118 mm × 118 mm) compared to the source of the illumination intensity (solar simulator), varying the incidence angle between 0° and 21° did not affect the "view" of the PV module. In fact, for each incidence angle, the PV module "sees" the source of light as being perpendicular. In addition, the open-circuit voltage is less sensitive to light intensity as pointed out by Chegaar et al. [52] and Wolf and Rauschenbach [53].

3.1.2. Comparison of Short-Circuit Current. Figure 6 shows the comparison of the short-circuit current of the three PV modules at each incidence angle. It can be seen that there was no substantial variation in the short-circuit current of the three PV modules at each incidence angle. This is due to the fact all the PV modules had identical parameters (irradiance, total surface area, and optical properties) that influence the generation of the short-circuit current. In the absences of series resistance effect, short-circuit current is a linear function of the light generated current which is proportional to the intensity [7, 54]. It can also be seen from Figure 6 that the short-circuit current of each PV module was constant at each incidence angle. This implies that there was no variation in the solar irradiance at each incidence angle.

3.1.3. Comparison of Maximum Power Output. The maximum power output of the three PV modules at each incidence

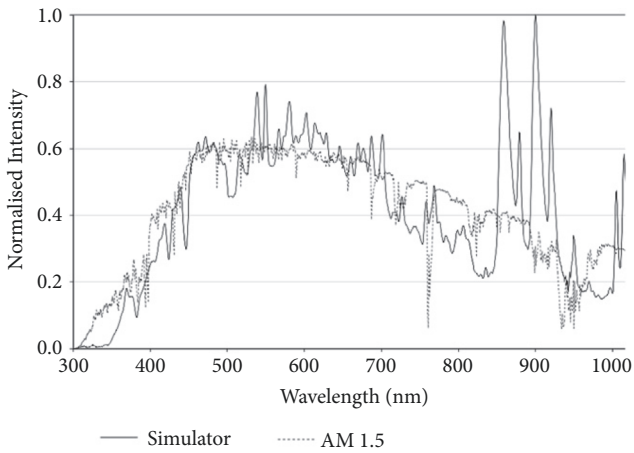

Figure 3: The multimobile solar simulator spectral distribution compared to the AM1.5 standard solar spectrum [29].

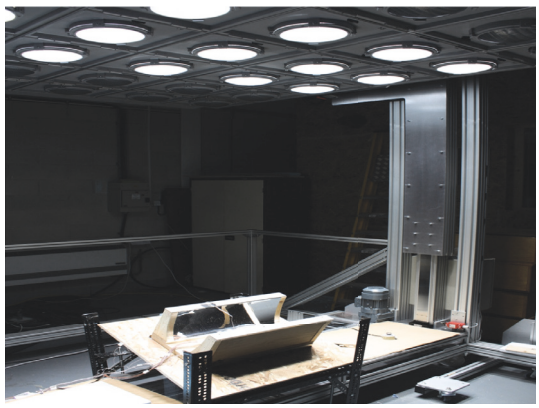

Figure 4: Experimental set up of one of the PV module with the CPC tilted at 15° from the perpendicular of the aperture of the collector.

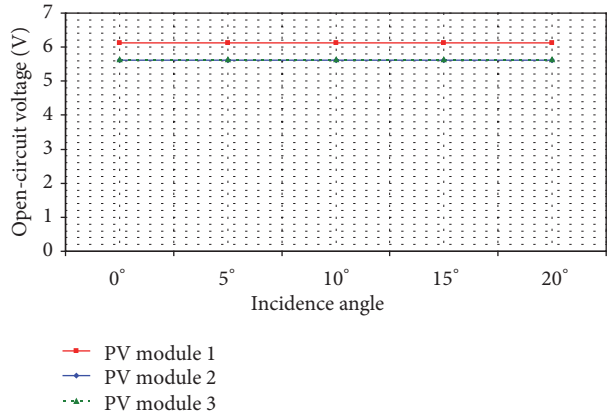

Figure 5: Comparison of open-circuit voltage of the three PV modules at various incidence angles.

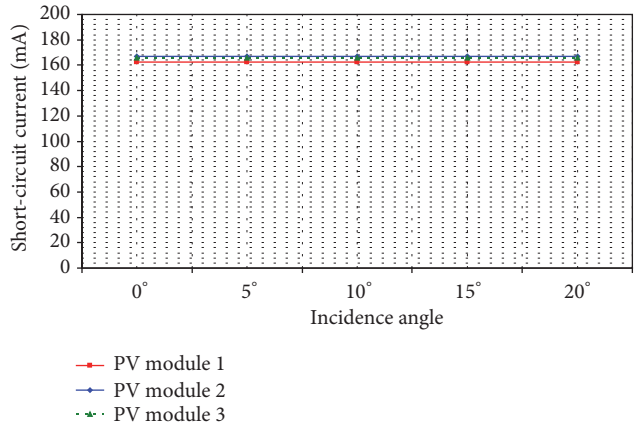

Figure 6: Comparison of short-circuit current of the three PV modules at each incidence angle.

angle is shown in Figure 7. It can be seen that the maximum power output of PV module 1 at each incidence angle was higher than that of PV module 2 and PV module 3 by about 7%. This result was expected because PV module 2 and PV module 3 were designed to take the advantage of the nonuniform illumination. PV modules 2 and 3 were designed in such a way that nonuniform illumination should affect only a group of cells but not the entire PV module. As illustrated in Figure 7, the maximum power output of each PV module was constant at each incidence angle because there was no variation in the illumination intensity, series resistance, and temperature that affect the power output.

In general, the total maximum power output of PV module 1 was higher than that of PV module 2 and PV module 3 by about 7%. Therefore, under uniform illumination (without concentrator), there is no need for special PV module design.

3.1.4. Comparison of Fill Factor. Figure 8 shows the comparison of the FF of the three PV modules at each incidence angle. It can be seen that all the PV modules had the same value (73%) of FF at each incidence angle. This is due to the fact that under uniform illumination, series resistance effect (which reduces the FF) is negligible [10, 54].

3.2. Electrical Performance Analysis of the PV Modules under Low Nonuniform Illumination. This section presents the results from the analysis when the PV modules were tested at low nonuniform illumination. Low nonuniform illumination was created by integrating the PV modules with the V-trough collector (Figure 2(a)). Figure 9 shows the magnitude and profile of the experimental energy flux distributions along the PV module with the V-trough collector for illumination intensity incident at 0°, 5°, 10°, 15°, and 20°. It can be seen that the energy flux distributions was nonuniform and the magnitude of illumination uniformity varied with incidence angle. However, the magnitude at any incidence angle never exceeded 2.7 which confirm that the PV modules were tested at low nonuniform illumination condition.

3.2.1. Comparison of Open-Circuit Voltage. Figure 10 compares the open-circuit voltage of the three PV modules at various incidence angles. It can be seen that the open-circuit voltage of PV module 1 was higher than that of PV module

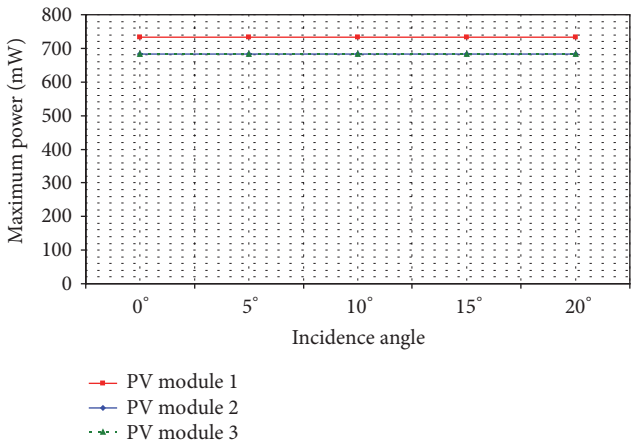

Figure 7: Comparison of maximum power output of the three PV modules at each incidence angle.

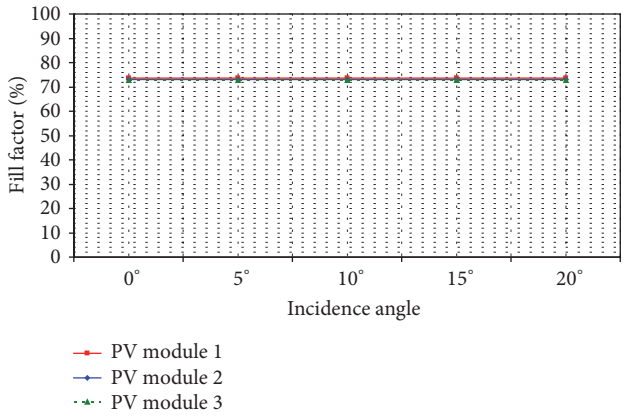

Figure 8: Comparison of fill factor of the three PV modules at various incidence angles.

2 and PV module 3 by about 8% nearly at each incidence angle. This is due to recombination effect as explained in Section 3.1.1. As illustrated in Figure 10, the open-circuit voltage of each PV module remained almost constant at each incidence angle. This is explained by the fact that the open-circuit voltage depends on neither the energy absorbed nor the energy flux distribution, but only on saturation current and light generated current [52, 53].

3.2.2. Comparison of Short-Circuit Current. The variation of short-circuit current of each PV module as a function of solar incidence angle is shown in Figure 11. It can be seen the value of the short-circuit current for the three PV modules was not constant due to nonuniform illumination at each incidence angle. However, the value of short-circuit current for PV module 1 was always less than that of PV module 2 and PV module 3 at each incidence angle. As illustrated in Figure 11, when the solar irradiance was incident perpendicular to the aperture of the V-trough collector, the value of the short-circuit current for PV module 3 was higher than that of PV module 2 and PV module 1 by about 3% and 27%, respectively. PV modules 2 and 3 had higher I_{SC} than PV module 1 because the current generated by PV module 1 was limited by the least-illuminated cells since all the cells were connected in series. On the other hand, PV module 3 had higher I_{SC} than PV module 2 because the peak energy concentration (between 34 mm and 54 mm) occurred in one group of cells in series connection with many solar cells (6) as compared to only 5 cells in PV module 2.

As illustrated in Figure 11, from 10° incidence angle and above, the values of the short-circuit current for PV module 2 were always higher than that of PV module 1 and PV module 3. This is due to the fact that PV module 2 had three groups of cells connected in series and at each incidence angle, the peak energy concentration occurred in one of the group. Thus, high short-circuit current at each incidence angle. However, for PV module 3 and PV module 1, high energy concentration was lost as the value of the short-circuit current was limited by the cells with the least energy flux concentration.

3.2.3. Comparison of Maximum Power Output. Figure 12 shows the variation of maximum power output of each PV module as a function of incidence angle. It can be seen that at 0° incidence angle, the maximum power output of PV module 2 was higher than that of PV module 1 and PV module 3 by about 7% and 8%, respectively. PV module 1 had lower value than PV module 2 because the maximum power output of the entire PV module was limited by the cells with the least energy flux concentration. On the other hand, PV module 3 had lower value than PV module 2 because the maximum power output from cells 1, 2, 3, 9, 10, and 11 which were connected in series (as one string) was limited by the cells with the least energy concentration (Figure 9(a)). At 5° and 10° incidence angles, PV module 1 had higher maximum power output that PV module 2 and PV module 3 because the size of the solar cells occupied by high energy peak was relatively small. Thus, PV module 2 and PV module 3 had no advantages over PV module 1. However, at 15° and 20° incidence angles, PV module 2 performed better than both PV module 1 and PV module 3.

In general, the total maximum power output of PV module 2 was higher than that of PV module 1 and PV module 3 by about 4% and 7%, respectively. This is due to the fact that PV module 2 had three groups of solar cells connected in series, hence less nonuniform illumination effect. Therefore, for concentrating collectors with low concentration ratios such as the V-trough, PV modules with groups of cells in series connection instead of all cells being connected in series provide maximum current generation and hence high power output.

3.2.4. Comparison of Fill Factor. Figure 13 shows the comparison of the FF of the three PV modules at various incidence angles. It can be seen that all the PV modules had high fill factor though the fill factor of PV module 1 was always higher than that of PV module 2 and PV module 3 at each incidence angle. The reason is that PV module 2 and PV module 3 (which utilise the peak energy concentration) had higher series resistance loss than PV module 1, thus more reduction in FF. The fill factor of a PV cell decreases with increase in

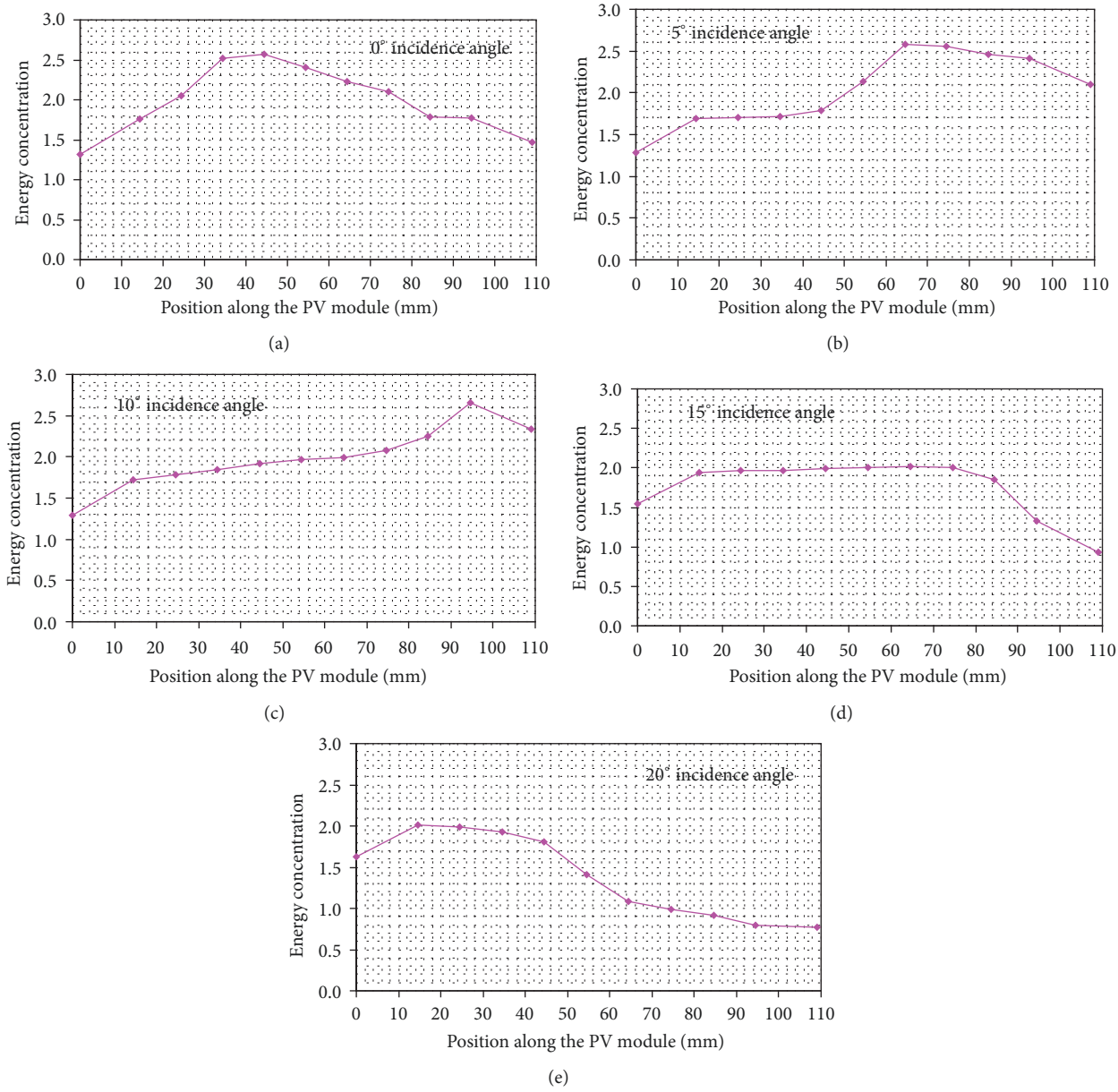

Figure 9: Experimental solar energy flux distributions along the PV module with the V-trough collector (a) 0°, (b) 5°, (c) 10°, (d) 15°, and (e) 20° incidence angle.

series resistance [54, 55]. In addition, series resistance effect is higher under nonuniform illumination condition than with uniform illumination [10]. As shown in Figure 13, there is no substantial difference between the fill factor for PV module 2 and PV module 3 because they had similar influence of series resistance.

3.3. Electrical Performance Analysis of the PV Modules under High Nonuniform Illumination. This section presents the results from the analysis when the PV modules were tested at high nonuniform illumination condition. In this work, high nonuniform illumination was created by integrating the PV module into the CPC (Figure 2(b)). Figure 14 shows the magnitude and profile of the experimental energy flux distributions along the PV module with the CPC for illumination intensity incident at 0°, 5°, 10°, 15°, and 20°. It can be seen that the energy flux distributions was nonuniform and the magnitude of illumination uniformity varied with the incidence angle. On the other hand, it can be seen that the CPC had high nonuniform energy flux concentration along the PV module than the V-trough collector (Figure 9).

3.3.1. Comparison of Open-Circuit Voltage. Figure 15 shows the variation in open-circuit voltage of the three PV modules as a function of incidence angle. As it was the cases of uniform and low nonuniform illumination, the open-circuit

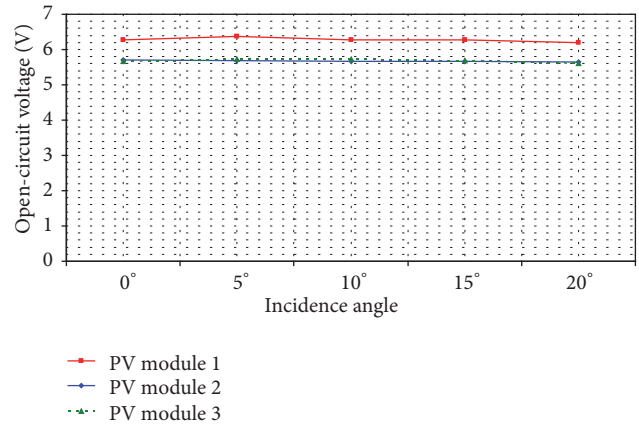

Figure 10: Comparison of open-circuit voltage of the three PV modules at each incidence angle.

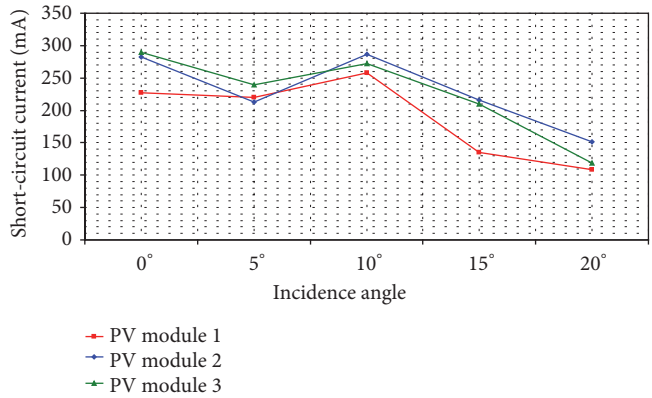

Figure 11: Comparison of short-circuit current of the three PV modules at various incidence angles.

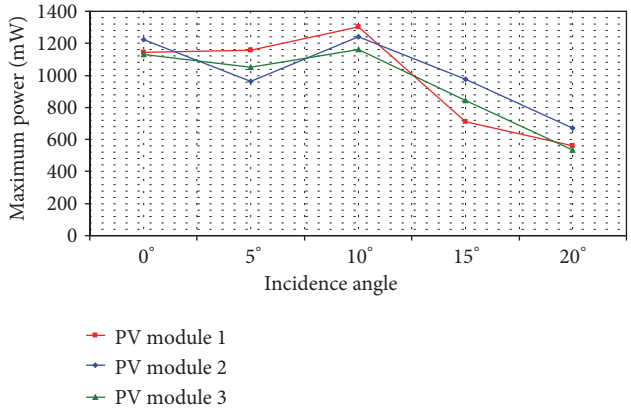

Figure 12: Comparison of maximum power output of the three PV modules at various incidence angles.

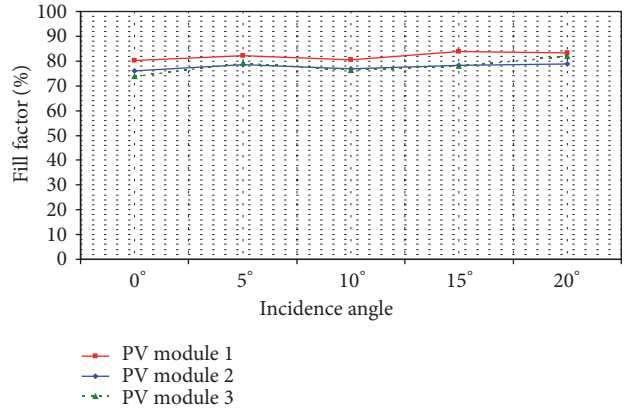

Figure 13: Variation of fill factor of each PV module as a function of incidence angle.

voltage of PV module 1 was always higher than that of PV module 2 and PV module 3 at each incidence angle. This is due to recombination effect as explained in Section 3.1.1. It can be observed from Figure 15 that when solar irradiance was incident perpendicular, the open-circuit voltage of PV module 1 was higher than that of PV module 2 and PV module 3 by about 7% and 21%, respectively. However, towards the acceptance angle limits of the CPC, the open-circuit voltage of PV module 1 was higher than that of PV module 2 and PV module 3 by about 10% and 11%. On the other hand, the open-circuit voltage of PV module 2 was slightly higher than that of PV module 3 at 0° incidence

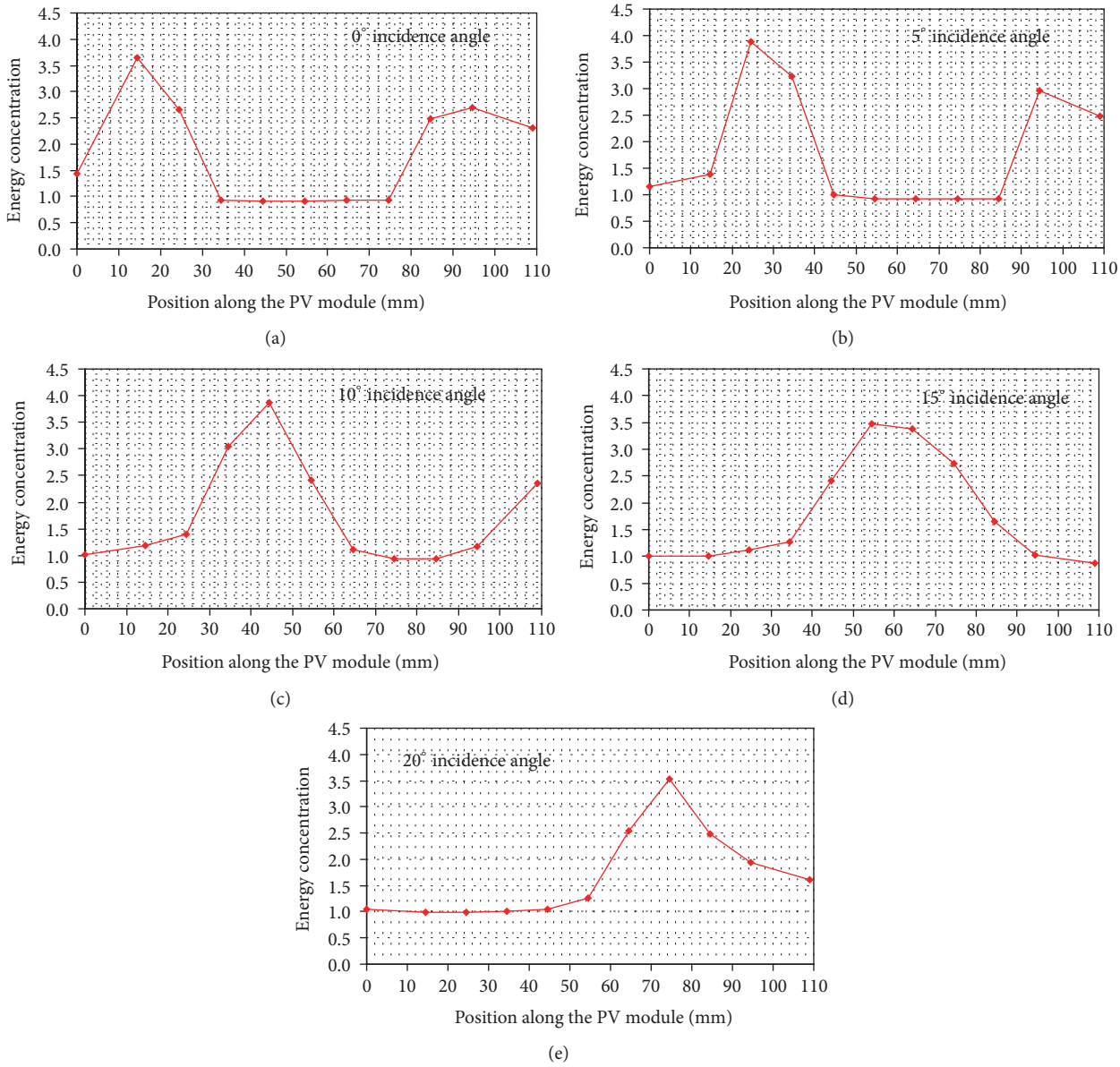

FIGURE 14: Experimental solar energy flux distributions along the PV module with the CPC (a) 0°, (b) 5°, (c) 10°, (d) 15°, and (e) 20° incidence angle.

angle and remained almost the same from 5° and above. As illustrated in Figure 15, the open-circuit voltage of each PV module (expect PV module 3 at 0°) remained almost constant due to the fact that it is less sensitive to light intensity.

3.3.2. Comparison of Short-Circuit Current. Figure 16 shows the variation in short-circuit current of the three PV modules at each incidence angle. Due to high nonuniform energy concentration at each incidence angle illustrated in Figure 14, the short-circuit current of each PV module was very high and nonuniform. On the other hand, the short-circuit current of PV module 2 and PV module 3 was always higher than that of PV module 1 due to the fact that the modules (PV module 2 and PV module 3) were designed to take the advantage of the effect of nonuniform illumination. When the illumination intensity was incident perpendicular to the aperture of the CPC (0°), the short-circuit current of PV module 3 was higher than that of PV module 2 and PV module 1 by about 9% and 86%, respectively. On the other hand, the short-circuit current of PV module 2 was higher than that of PV module 1 by about 70%. This is due to the fact that the short-circuit current for PV module 1 was limited by the cells with the least energy concentration whereas, for PV modules 2 and 3, the effect of nonuniform illumination resulted in high short-circuit currents. It has been found that a PV module with isolated cells operate efficiently for the reason that each cell performs to its potential as the generated current is no longer limited by the least illuminated cell(s) [7].

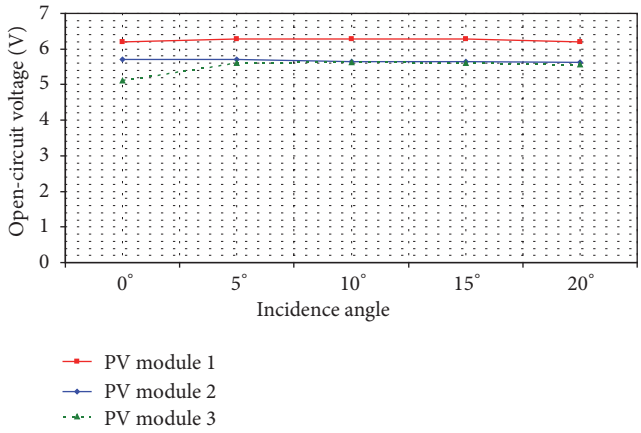

Figure 15: Variation of open-circuit voltage of each PV module as a function of incidence angle.

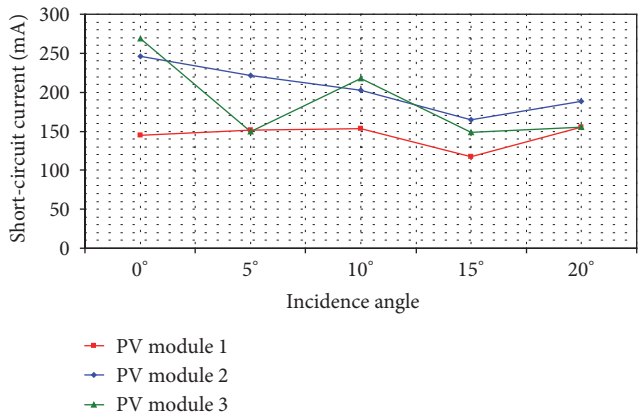

Figure 16: Variation of short-circuit current of each PV module as a function of incidence angle.

As illustrated in Figure 16, when the illumination intensity was incident at 5° from the perpendicular of the aperture of the CPC, the short-circuit current of PV module 2 was higher than that of PV module 3 and PV module 1 by about 47%. For PV module 1, this was due to the effect of nonuniform illumination as the short-circuit current of the entire PV module was limited by the least illuminated cells. However, PV module 3 had lower value of short-circuit current than PV module 2 because at this angle both groups of solar cells (group 1 with cells 1, 2, 3, 9, 10, and 11 in series and group 2 with cells 4, 5, 6, 7, and 8 in series) were in the lowest energy concentration region (Figure 14(b)). Short-circuit current is a linear function of the light generated current which is proportional to the photon flux incident on the PV cell; thus PV cells in the lowest energy regions produce less current than those in the peak energy concentration regions [7]. Similar explanations apply for the results at other incidence angles.

From Figure 16, it can be seen that the short-circuit current of each module decreased with the increase in incidence angle. This is due to the fact that an increase in incidence angle results in solar irradiance reduction.

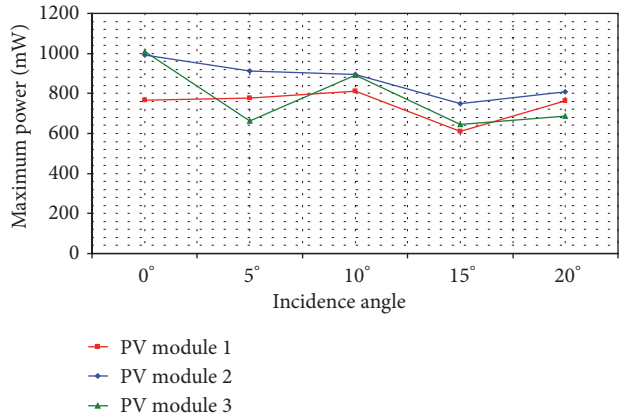

Figure 17: Variation of maximum power output of each PV module as a function of incidence angle.

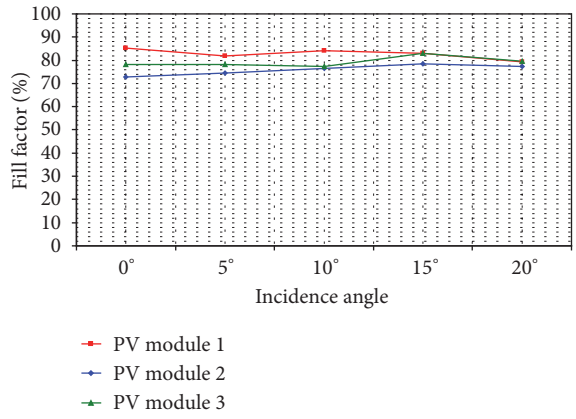

Figure 18: Variation in fill factor of each PV module as a function of incidence angle.

3.3.3. Comparison of Maximum Power Output. Figure 17 shows the variation in maximum power output of each PV module as a function of incidence angle. It can be seen that the maximum power output of each module was not uniform due to variation in energy flux concentration (Figure 14) as a result of nonuniform illumination and angular dependent effect. On the other hand, the maximum power output of PV module 2 was always higher than that of PV module 1 at each incidence angle. For example, when the illumination intensity was incident at 0°, 5°, 10°, 15°, and 20° from the perpendicular of the aperture of the CPC, the maximum power output of PV module 2 was higher that of PV module 1 by about 30%, 17%, 10%, 23%, and 6%, respectively. This was due to the effect of nonuniform illumination as the maximum power of PV module 1 was limited by the least illuminated cells. At 0° and 10° incidence angles, both PV module 2 and PV module 3 had the same value of maximum power output. However, at 5°, 15°, and 20° incidence angles, the maximum power output of PV module 2 was higher than that of PV module 3 by about 37%, 16%, and 18%, respectively. At these angles, PV module 3 was not as effective as PV module 2 because at these angles both groups of solar cells (group 1 with cells 1, 2, 3, 9, 10, and 11 in series and group 2 with cells 4, 5, 6, 7, and 8 in series) were in

the lowest energy concentration region (Figures 14(b), 14(d), and 14(e)), which means lower power output than that of PV module 2. On the other hand, the maximum power output of PV module 3 was higher than that of PV module 1 only at 0°, 10°, and 15° incidence angles.

From Figure 17, it can be seen that the maximum power output of each module decreased with the increase in incidence angle. This is due to the fact that an increase in incidence angle results in solar irradiance reduction (power output has a linear relationship with solar radiation intensity similar to short-circuit current).

In general, the total maximum power output of PV module 2 was higher than that of PV module 3 and PV module 1 by about 12% and 17%, respectively. This is due to the fact that the effect of nonuniform illumination was significant in PV module 3 than in PV module 2 because PV module 2 had three groups of cells in series connection while PV module 3 had two groups of cells in series connection. Therefore, the best PV module design at high nonuniform illumination was PV module 2. In practical situation this indicates that PV module manufacturers should consider manufacturing PV modules with groups of cells in series connection instead of having all cells connected in series.

3.3.4. Comparison of Fill Factor. Figure 18 illustrates the variation in fill factor for each PV module as a function of incidence angle. It can be seen that all the PV modules had high fill factor (between 73% and 85%); however, the fill factor of PV module 1 was always higher than that of PV module 2 and PV module 3 at each incidence angle. This can be explained by the dominance of recombination mechanism in the space-charge region which increased the ideality factor and series resistance losses at higher energy flux. The same reasons apply for the observed differences between PV module 2 and PV module 3.

4. Conclusions

In this study, three different PV modules with cells connected in different configurations to address nonuniform illumination effect in solar collectors were investigated. The electrical parameters (open-circuit voltage, short-circuit current, maximum power output, and fill factor) of each PV module were analysed at uniform and nonuniform illumination conditions. The uniform solar radiation illumination was achieved by testing the PV modules at solar simulator without concentrating system whilst nonuniform illumination was created by testing the PV modules with the V-trough collector (low non-uniform illumination) and the CPC (high nonuniform illumination). When the PV modules were tested at uniform illumination, the total maximum power output of PV module 1 was higher than that of PV module 2 and PV module 3 by about 7%. Therefore, PV module 2 and PV module 3 had no advantage of standard PV module at uniform illumination. However, when the PV modules were tested at low nonuniform illumination, the total maximum power output of PV module 2 was higher than that of PV module 1 and PV module 3 by about 4% and 7%, respectively. This difference increased to about 12% for PV module 3 and 17% for PV module 1 when modules were tested at high nonuniform illumination within the CPC. Therefore, the best PV module design to address nonuniform illumination effect in solar collector is PV module 2. In practical situation this implies that manufacturers of PV modules should consider designing PV modules with groups of cells in series connection instead of all cells being in series connection.

Nomenclature

I_{MPP}:	Current at maximum power output [A]
I_{SC}:	Short–circuit current [A]
J_0:	Reverse saturation current density [A/cm^2]
J_{ph}:	Photo-current density [A/cm^2]
k_B:	Boltzmann constant [J/K]
P_{MPP}:	Power output at maximum power point [W]
PV module 1:	PV module in which 11 solar cells are connected in series
PV module 2:	PV module in which 11 solar cells are connected in three blocks as follows: block 1: solar cells numbers 1, 2, and 3 are connected in series; block 2: solar cells numbers 4, 5, 6, 7, and 8 are connected in series and block 3: solar cells numbers 9, 10, and 11 are connected in series.
PV module 3:	PV module in which 11 solar cells are connected in two blocks as follows: block 1: solar cells numbers 1, 2, 3, 9, 10, and 11 are connected in series and block 2: solar cells numbers 4, 5, 6, 7, and 8 are connected in series.
q:	Absolute value of the electron charge [C]
T:	Absolute temperature [K]
V_{MPP}:	Voltage at maximum power point [V]
V_{OC}:	Open-circuit voltage [V]

Greek

η: Solar cell conversion efficiency [-]

Abbreviations

2D:	Two-dimensional
3D:	Three-dimensional
AM:	Air mass
CPC:	Compound parabolic concentrator
FF:	Fill factor
I–V:	Current versus voltage
PV:	Photovoltaic
PV-CPC:	Photovoltaic-compound parabolic concentrator
WD-CPC:	Well distributed compound parabolic concentrator.

Data Availability

The data may be submitted if required.

Conflicts of Interest

The author declares that they have no conflicts of interest.

Acknowledgments

The author wishes to thank Chosun University (Republic of Korea) for their financial support. Indeed, without this funding, this article would have not been written.

References

[1] R. Tang and X. Liu, "Optical performance and design optimization of V-trough concentrators for photovoltaic applications," *Solar Energy*, vol. 85, no. 9, pp. 2154–2166, 2011.

[2] V. V. Tyagi, N. A. A. Rahim, and J. A. L. Selvaraj, "Progress in solar PV technology: research and achievement," *Renewable & Sustainable Energy Reviews*, vol. 20, pp. 443–461, 2013.

[3] E. L. Ralph, "Use of concentrated sunlight with solar cells for terrestrial applications," *Solar Energy*, vol. 10, no. 2, pp. 67–71, 1966.

[4] D. Chemisana and T. K. Mallick, "Building integrated concentrating solar systems," *Solar Energy Sciences and Engineering Applications*, pp. 508–552, 2013.

[5] J. Sangrador and G. Sala, "Static concentrators for two-sided photovoltaic solar cells," *Solar Energy*, vol. 23, no. 1, pp. 53–60, 1979.

[6] H. Baig, K. C. Heasman, and T. K. Mallick, "Non-uniform illumination in concentrating solar cells," *Renewable & Sustainable Energy Reviews*, vol. 16, no. 8, pp. 5890–5909, 2012.

[7] D. I. Paul, M. Smyth, A. Zacharopoulos, and J. Mondol, "The design, fabrication and indoor experimental characterisation of an isolated cell photovoltaic module," *Solar Energy*, vol. 88, pp. 1–12, 2013.

[8] D. I. Paul, "Theoretical and experimental optical evaluation and comparison of symmetric 2D CPC and V-trough collector for photovoltaic applications," *International Journal of Photoenergy*, vol. 2015, Article ID 693463, 13 pages, 2015.

[9] R. Ramabadran and B. Mathur, "Effect of shading on series and parallel connected solar PV modules," *Modern Applied Science (MAS)*, vol. 3, no. 10, pp. 32–41, 2009.

[10] C. Garner and R. Nasby, "Effects of nonuniform illumination on the performance of silicon concentrator solar cells," in *Proceedings of the 25th IEEE International Electron Devices Meeting (IEDM 1979)*, pp. 312-313, Washington, DC, USA, 1979.

[11] A. Cuevas and S. López-Romero, "The combined effect of nonuniform illumination and series resistance on the open-circuit voltage of solar cells," *Solar Cells*, vol. 11, no. 2, pp. 163–173, 1984.

[12] V. Quaschning and R. Hanitsch, "Numerical simulation of current-voltage characteristics of photovoltaic systems with shaded solar cells," *Solar Energy*, vol. 56, no. 6, pp. 513–520, 1996.

[13] L. W. James and J. K. Williams, "Fresnel optics for solar concentration on photovoltaic cells," in *Proceedings of the 13th IEEE Photovoltaic Specialists Conferences*, pp. 673–679, Washington, DC, USA, 1978.

[14] M. W. Edenburn and J. R. Burns, "Shading analysis of a photovoltaic cell string illuminated by a parabolic through concentrator," in *Proceedings of the 15th IEEE Photovoltaic Specialists Conference, May 12–15*, pp. 63–68, Kissimmee, Florida, USA, 1981.

[15] D. I. Paul, A. Zacharopoulos, and M. Smyth, "The effect of non-uniformities in temperature on the performance parameters of an isolated cell photovoltaic module with a compound parabolic concentrator," *International Journal of Renewable Energy Technology*, vol. 10, no. 1/2, pp. 3–25, 2019.

[16] E. L. Burgess, "Photovoltaic energy conversion using concentrated sunlight," in *Proceedings of Photo-Optical Instrumentation Engineers (SPIE) 0085. Solar Energy Utilization II*, pp. 9–15, San Diego, USA, 1976.

[17] J. Gorski, R. L. Cole, R. M. Graven, W. Melntire, R. Schertz, R. Winston et al., "Photovoltaic power generation by use of compound parabolic concentrators," in *Proceedings of Condensed Papers Miami International on Conference on Alternative Energy Sources*, T. N. Veziroglu, Ed., pp. 787–789, Florida, USA, 1977.

[18] A. Rabl, "Comparison of solar concentrators," *Solar Energy*, vol. 18, no. 2, pp. 93–111, 1976.

[19] P. Bendt, A. Rabl, H. W. Gaul, and K. A. Reed, "Optical analysis and optimization of line focus solar collectors," Task No.3432.30, Contract No. EG.77.C.01.4042, Solar Energy Research Institute, U.S. Department of Energy, 1979.

[20] I. Zanesco and E. Lorenzo, "Optimisation of an asymmetric static concentrator: the PEC-44D," *Progress in Photovoltaics*, vol. 10, no. 5, pp. 361–376, 2002.

[21] A. Rabl, "Optical and thermal properties of compound parabolic concentrators," *Solar Energy*, vol. 18, no. 6, pp. 497–511, 1976.

[22] A. Rabl and R. Winston, "Ideal concentrators for finite sources and restricted exit angles," *Applied Optics*, vol. 15, no. 11, pp. 2880–2883, 1976.

[23] A. Zacharopoulos, DI. Paul, J. Mondol, and M. Smyth, "Optical characterisation of a PV concentrator under simulated and realistic solar conditions using an isolated cell PV module," in *Proceedings of the Eurosun2012 Conference; 2012 September 18–20*, Opatija, Croatia, 2012.

[24] N. Sarmah, B. S. Richards, and T. K. Mallick, "Evaluation and optimization of the optical performance of low-concentrating dielectric compound parabolic concentrator using ray-tracing methods," *Applied Optics*, vol. 50, no. 19, pp. 3303–3310, 2011.

[25] G. Li, Q. Xuan, Y. Lu, G. Pei, Y. Su, and J. Ji, "Numerical and lab experiment study of a novel concentrating PV with uniform flux distribution," *Solar Energy Materials & Solar Cells*, vol. 179, pp. 1–9, 2018.

[26] A. Gupta, K. S. Murlidhar, and V. K. Tewery, "Design and testing of a uniformly illumination non-tracking concentrator," *Sol Energy*, vol. 27, no. 5, pp. 387–391, 1981.

[27] Y. Yu, R. Tang, and C. Xia, "Irradiation distribution on solar cells inside CPCs with a restricted exit angle," *Advanced Materials Research*, vol. 588-589, pp. 603–607, 2012.

[28] H. Zhang, H. Chen, Y. Han, H. Liu, and M. Li, "Experimental and simulation studies on a novel compound parabolic concentrator," *Journal of Renewable Energy*, vol. 113, pp. 784–794, 2017.

[29] A. Zacharopoulos, J. D. Mondol, M. Smyth, T. Hyde, and V. O'Brien, "State-of-the-art solar simulator with dimming control and flexible mounting," in *Proceedings of the 29th Biennial Solar World Congress of the International Solar Energy Society (ISES '09)*, pp. 854–863, Johannesburg, South Africa, October 2009.

[30] J. Nilsson, R. Leutz, and B. Karlsson, "Micro-structured reflector surfaces for a stationary asymmetric parabolic solar concentrator," *Solar Energy Materials & Solar Cells*, vol. 91, no. 6, pp. 525–533, 2007.

[31] S. Hatwaambo, H. Hakansson, J. Nilsson, and B. Karlsson, "Angular characterization of low concentrating PV-CPC using low-cost reflectors," *Solar Energy Materials & Solar Cells*, vol. 92, no. 11, pp. 1347–1351, 2008.

[32] S. Hatwaambo, H. Hakansson, A. Roos, and B. Karlsson, "Mitigating the non-uniform illumination in low concentrating CPCs using structured reflectors," *Solar Energy Materials & Solar Cells*, vol. 93, no. 11, pp. 2020–2024, 2009.

[33] S. Hatwaambo, "Performance analysis of low concentrating PV-CPC systems withstructured reflectors," in *Solar Power*, R. Rugescu, Ed., pp. 212–222, 2009, http://cdn.intechweb.org/pdfs/28486.pdf.

[34] J. Simfukwe, S. Hatwaambo, and K. Hansingo, "Using structured aluminum reflectors in flux scattering on module performance," in *Proceedings of the World Renewable Energy Congress – Sweden, 8–13 May, 2011*, pp. 2924–2929, Linköping, Sweden, 2011.

[35] D. Esparza, R. Rodríguez-Vera, R. Díaz-Uribe, and I. Moreno, "Solar concentrator with diffuser segments," in *Proceedings of SPIE (Society of Photo-Optical Instrumentation Engineers)*, R. Rodríguez-Vera and R. Díaz-Uribe, Eds., The 22nd Congress of the International Commission for Optics: Light for the Development of the World, Puebla, Mexico, 2011.

[36] A. Parretta, G. C. Righini, A. Consortini et al., "Modelling of CPC-based photovoltaic concentrator," in *Proceedings of the 19th Congress of the International Commission for Optics: Optics for the Quality of Life*, vol. 4829, pp. 1045–1047, Firenze, Italy.

[37] C. A. F. Fernandes, J. P. N. Torres, P. J. C. Branco, J. Fernandes, and J. Gomes, "Cell string layout in solar photovoltaic collectors," *Energy Conversion and Management*, vol. 149, pp. 997–1009, 2017.

[38] D. I. Paul and M. Smyth, "Enhancing the performance of a building integrated compound parabolic photovoltaic concentrator using a hybrid photovoltaic cell," *International Journal of Renewable Energy Technology*, 2018.

[39] K. D. Mannan and R. B. Bannerot, "Optimal geometries for one- and two-faced symmetric side-wall booster mirrors," *Solar Energy*, vol. 21, no. 5, pp. 385–391, 1978.

[40] G. Jorgensen and T. Wendelin, *Uniform Flux Dish Concentrators for PV Application*, National Renewable Energy Laboratory, NREL/TP441-4800, U.S. Department of Energy, Colorado, USA, 1992.

[41] P. Singh and J. A. Liburdy, "A solar concentrator design for uniform flux on a flat receiver," *Energy Conversion and Management*, vol. 34, no. 7, pp. 533–543, 1993.

[42] N. Fraidenraich, "Design procedure of V-trough cavities for photovoltaic systems," *Progress in Photovoltaics*, vol. 6, no. 1, pp. 43–54, 1998.

[43] D. I. Paul, *Characterisation of solar concentrating systems for photovoltaics and their impact on performance [Ph.D. thesis]*, University of Ulster, UK, 2011.

[44] Anon, *CM4 High Temperature Pyranometer User Manual Version 0706. Kipp and Zonen B.V*, Delftechpark, Delft Holland, The Netherland, 2003.

[45] Anon, *2400 Series SourceMeter® User's Manual, Seventh Printing, Document Number: 2400S-900-01 Rev. G*, Inc. Cleveland, Ohio, USA, 1999.

[46] M. A. Green, *Solar Cells: Operating Principles, Technology and System Applications*, The University of New South Wales, Kensington, Australia, 1992.

[47] A. S. Blazev, *Photovoltaics for Commercial and Utilities Power Generation*, Fairmont Press, Florida, USA, 2012.

[48] S. Adhikari, B. Majhi, and A. K. Bandyopadhya, "Photovoltaic effect and solar energy: a brief perspectivePart II," *Kach (Journal of the all India Glass Manufacturers Federation)*, vol. 3, no. 2, pp. 41–44, 2015.

[49] W. Shockley and H. J. Queisser, "Detailed balance limit of efficiency of p-n junction solar cells," *Journal of Applied Physics*, vol. 32, no. 3, pp. 510–519, 1961.

[50] A. Luque and A. Martí, "Increasing the efficiency of ideal solar cells by photon induced transitions at intermediate levels," *Physical Review Letters*, vol. 78, no. 26, pp. 5014–5017, 1997.

[51] O. Breitenstein, "Understanding the current-voltage characteristics of industrial crystalline silicon solar cells by considering inhomogeneous current distributions," *Opto-Electronics Review*, vol. 21, no. 3, pp. 259–282, 2013.

[52] V. M. Andreev, V. A. Grilikhes, and V. D. Rumyantsev, *Photovoltaic Conversion of Concentrated Sunlight*, John Wiley and Sons, Chichester, UK, 1997.

[53] M. Chegaar, P. Petit, A. Hamzaoui, M. Aillerie, A. Namoda, and A. Herguth, "Effect of illumination intensity on solar cells parameters," *Energy Procedia*, vol. 36, pp. 722–729, 2013.

[54] M. Wolf and H. Rauschenbach, "Series resistance effects on solar cell measurements," *Advanced Energy Conversion*, vol. 3, no. 2, pp. 455–479, 1963.

[55] S. Bowden and A. Rohatgi, "A rapid accurate determination of series resistance and fill factor losses in industrial silicon solar cells," in *Proceedings of 17th European Photovoltaic Solar Energy Conference*, pp. 1802–1806, 2001.